Recent developments on fractal-based approach to nanofluids and nanoparticle aggregation

Jianchao Cai[1], Xiangyun Hu[1*], Boqi Xiao[2*], Yingfang Zhou[3], Wei Wei[1]

1 Hubei Subsurface Multi-scale Imaging Key Laboratory, Institute of Geophysics and Geomatics, China University of Geosciences, Wuhan 430074, P.R. China;

2 School of Mechanical and Electrical Engineering, Sanming University, Sanming 365004, P.R. China;

3 School of Engineering, University of Aberdeen, FN 264, King's College, Aberdeen, AB24 3UE, the UK

* Corresponding Author.

Email:

caijc@cug.edu.cn (J. Cai), xyhu@cug.edu.cn (X. Hu), mr.boqi-xiao@connect.polyu.hk (B. Xiao)

Abstract

The properties of nanoparticles and its aggregation as well as convective heat transfer of nanofluids have received great attentions over the last few decades. It is well certified that nanoparticles and its aggregation can be successfully described by fractal geometry theory and technology. In this review, the fractal properties of nanoparticle and its aggregation are firstly introduced, and then the recent investigations on the fractal models and fractal-based approaches that applied for effective thermal conductivity, convective heat transfer, critical heat flux and subcooled pool boiling of nanofluids, fractal clusters and yield stress property of nanoparticle aggregation are summarized.

Keywords: nanoparticle aggregation, fractal, nanofluids, thermal conductivity, convective heat transfer

Note: words/sentences/paragraphs in BLUE indicate revisions or newly-added material.

Content

1. Introduction of nanoparticle and fractal geometry

Nanoparticles are ultrafine particles, in which the particle is thought as a small object that behaves as a whole unit of its transport and properties. Since the unique properties of the nanoscale, nanoparticles have been extensively used in a variety of applications, such as medicine, optics, electronics, manufacturing, materials, solar cells and catalysts [1-6]. Fluids with suspended nanoparticles are termed as nanofluids by Choi and Eastman [7]. There is a growing interest in experimental, theoretical and numerical investigations on yield stress property of nanoparticle aggregate and the thermal conductivity of nanofluids from theoretical perspectives to engineering applied science[8-11].

There are different views about the effect of nanoparticles on the fluid composites. On one hand, a large amount of works reported that the effective thermal conductivity of liquids with suspension of nanoparticles are anomalously larger than that of conventionally nanoparticle free heat transfer fluids [12-18]. Recently, Keblinski et al. [19] summarized how the relative increase in the thermal conductivity as a function of the volume fraction of nanoparticles reported in a wide range of published papers. Also see Table 1, in which some lager enhancement of 4-40% over a volume fraction of 0.1-5%, or even at lower particle loading, such as enhancement of 21% at 0.00026% of volume fraction can be found [20]. On the other hand, some studies do not exhibit anomalous enhancements of the thermal conductivity. For instance, Putnam et al. [21] experimentally observed that the largest increase in thermal conductivity is 1.3% for Au particles of diameter 4 nm suspended in ethanol at the volume fraction of 0.018%. Utomo et al. [22] found that TiO_2 and Al_2O_3 nanofluids do not show unusual enhancement in thermal conductivity. Buongiorno et al. [23] performed a study of nanofluids using a variety of experimental approaches, and their results suggested that nanoparticles could not enhance the thermal conductivity substantially. Hence it can be seen that the intrinsic mechanism for enhancement in the thermal conductivity of nanofluids should be further analysed from theoretical aspect.

Here insert Table 1

However, the macroscopic theory of heat transport in composite materials is failed to nanofluids [21, 37-40], such as effective medium theory. And thus a generally accepted theory or modelling for explaining the mechanisms of enhancing thermal conductivity using nanoparticles is necessary [41-47]. Keblinski et al. [48] suggested that the particle size, liquid-particle interface and the clustering of nanoparticles are major enhancement factors compared to Brownian motion of nanoparticles. They also pointed out that it is important to characterize the distribution of nanoparticles in liquid

by scattering technique. A complete particle distribution function is essential for evaluating the enhancement of thermal conductivity that produced by the coherent heat transport between particles separated by thin liquid layers [49-52].

As claimed by some researchers, the uniform distribution assumption is not capability to characterize most behaviours of nanoparticle aggregation [53, 54]. In reality, particles in nanofluids normally have different sizes, and some particles may contact each other to form clusters of different sizes [55, 56]. The theory of fractals aids in analysing the response of practical systems besides examining the complex geometries of nature. The nanoparticles in nanofluids have been proven to be fractal objects and the distribution of nanoparticles in suspension exhibits the fractal property [28, 55, 57-59]. The fractal dimensions of clustering CuO nanoparticles in water with different volume concentration are calculated based on Eq. (1) is 1.73 and 1.76 [28]. Havlin and Ben-Avraham [58] indicated that the size distributions of nanoparticles and nanoparticles in suspension were shown certain degree of self-similarity. This means that the fractal theory may be used to predict transport property of nanofluids. Wang et al. [28] experimentally found that the size of nanoparticles and its clusters follows fractal distribution, and developed a fractal model for predicting the effective thermal conductivity of liquid with nanoparticle inclusion. By means of fractal geometry, Xu et al. [57] proposed a model for heat convection due to the Brownian motion of nanoparticles, Xiao et al. [59] further improved Xu's model [57] and obtained a novel form of thermal conductivity of nanofluids with Brownian motion effect.

The fractal theory is developed in the 1980's [60] and is widely applied to many fields [61-67]. The mass of a fractal object (M) is related to measured scale ε through fractal dimension (D):

$$M(\varepsilon) \sim \varepsilon^{D} \tag{1}$$

Besides the exact self-similar fractals, many objects in nature are statistically self-similar fractals. The former exhibit the self-similarity over an infinite range of length scales, however, the latter usually exhibit the self-similarity in some average sense and over a certain local range of length scales (called prefractals).

The size distribution of nanoparticles in nanofluids, analogous to pores in fractal porous media, follows the fractal power law [28]. Thus, the number of particles whose sizes are within the infinitesimal range from λ to $\lambda + d\lambda$ is [68, 69]:

$$dN = -D\frac{\lambda_{\max}^{D}}{\lambda^{D+1}}d\lambda \tag{2}$$

and the probability density function $f(\lambda)$ for particles is given by [69]

$$f(\lambda) = D\frac{\lambda_{\min}^{D}}{\lambda^{D+1}} \qquad \lambda_{\min} \leq \lambda \leq \lambda_{\max} \tag{3}$$

where λ is the particle diameter, $\lambda_{\min}$ and $\lambda_{\max}$ are the minimum and maximum diameters of nanoparticles, respectively. The fractal dimension D can be measured by Box-counting method or be determined by [70]:

$$D = d_E - \frac{\ln\phi_p}{\ln\xi} \tag{4}$$

where d_E=2 in two dimensions, ϕ_p is the volume fraction of (primary) nanoparticles, ratio $\xi = \lambda_{\min}/\lambda_{\max}$ is assigned for simplification of formula writing. However, the limitation of fractal theory for nanofluids and nanoparticle aggregation is that the fractal theory must satisfy $\xi \leq 10^{-2}$. So, the fractal theory can be used to analyze the characters of nanofluids and nanoparticle aggregation.

The average diameter λ_{av} of nanoparticles can be decided based on the statistical property of fractal media, i.e:

$$\lambda_{av} = \int_{\lambda_{\min}}^{\lambda_{\max}} \lambda f(\lambda)d\lambda = \frac{D\lambda_{\max}}{D-1}\xi \tag{5}$$

Rewriting Eq.(5), the minimum and maximum nanoparticle diameter can be respectively obtained. From Eqs. (4) and (5), the ratio ξ is an important parameter for analysing the properties of nanoparticles by means of fractal geometry. Once ξ, ϕ_p and λ_{av} are measured, the D can be calculated by Eq. (4). Feng et al. [71] compared the values of D calculated by Eq. (4) with the experimental data by several investigators and found that the ratio of $\xi = 10^{-3}$ best fits the experimental data for different porous media. Similar conclusions can be also found in other applications of fractal theory [66, 72-74]. Considering that the pores in porous media are analogous to the particles in nanofluids, Eq. (4) was used to describe the particles in nanofluids and the ratio of $\xi = 10^{-3}$ was applied to analyse the heat conduction of nanofluids [57, 59, 75].

2. Fractal model for thermal conductivity of nanofluids

Two portions were normally considered as the main contribution to the heat transfer of nanofluids; there are heat transferred by stationary nanoparticles and the heat convection caused by moving nanoparticles, and the total effective thermal conductivity k_{eff} is hence expressed as:

$$k_{eff} = k_s + k_c \tag{6}$$

where k_c is the thermal conductivity by heat convection caused by Brownian motion of nanoparticles and k_s is the thermal conductivity by stationary nanoparticles in the liquid, which is simulated by the Maxwell-Garnett (MG) model. For the spherical-particle suspensions, the MG model gives [76]:

$$\frac{k_s}{k_f} = \frac{k_p + 2k_f - 2\phi_p(k_f - k_p)}{k_p + 2k_f + \phi_p(k_f - k_p)} \tag{7}$$

where k_p and k_f are the thermal conductivities of particles and fluid (host medium), respectively. The MG model is applicable to liquid with suspension of low concentration particle, and can be fit well with experimental results for randomly distributed and dilute components included in homogeneous host media, the suspended particles are thought as isolated in liquid and no interaction exists among them [28].

Recent experimental studies have shown that molecules those close to a solid surface in normal liquids organize into layered structures as similar to a solid [77]. Furthermore, there is an evidence that such an organized solid-like structure of a liquid at the surface is a governing factor in heat conduction from a solid wall to an adjacent liquid [78]. Therefore, Choi and coworkers [79] postulated that this organized solid/liquid interfacial shell makes the transport of energy across the interface effectively. Because the interfacial shells exist between the nanoparticles and the liquid matrix, both the interfacial shell and the nanoparticle can be regarded as a "complex nanoparticle". Therefore, the nanofluid system should be regarded as the complex nanoparticles dispersed in the fluid.

Xue [80] proposed a formula of calculating the thermal conductivity component along an axis of a complex rotational elliptical particle [48]. He assumed that the complex rotational nanoparticle was composed of a rotational elliptical nanoparticle of thermal conductivity k_p with half radii of (a, b, b)[1] and an elliptical shell of thermal conductivity k_{int} with a thickness of l. The thermal conductivity component along a and b axes of the complex rotational elliptical particle is expressed as:

$$k_{c,a} = k_{int} \frac{(1-B)k_{int} + Bk_p + \beta(1-B)(k_p - k_{int})}{(1-B)k_{int} + Bk_p - B\beta(k_p - k_{int})} \tag{8}$$

---

[1] Three axis of elliptical nanoparticle is (x, y, z), here the half radii $y=z=b$ is assumed for simplification

$$k_{c,b} = k_{int} \frac{(1+B)k_{int} + (1-B)k_p + (1+B)\lambda'(k_p - k_{int})}{(1+B)k_{int} + (1-B)k_p - (1-B)\lambda'(k_p - k_{int})} \qquad (9)$$

where $\beta = \dfrac{ab^2}{(a+l)(b+l)^2}$, B is the depolarization factor component of the rotational

elliptical particle along the long axis (a axis), $B = \dfrac{ab^2}{2} \displaystyle\int_0^\infty \dfrac{du}{(u+a^2)(u+b^2)\sqrt{u+a^2}}$.

According to the average theory, the equation for the effective thermal conductivity of the complex rotational elliptical particles dispersed nanofluid is proposed as:

$$9\left(1 - \frac{\phi_p}{\lambda'}\right)\frac{k_{eff} - k_f}{2k_{eff} + k_f} + \frac{\phi_p}{\beta}\left[\frac{k_{eff} - k_{c,a}}{k_{eff} + B(k_{c,a} - k_{eff})} + \frac{4(k_{eff} - k_{c,b})}{2k_{eff} + (1-B)(k_{c,b} - k_{eff})}\right] = 0 \qquad (10)$$

When the dispersed particles are spheres, Eq. (10) reduces to [81]

$$\left(1 - \frac{\phi_p}{\beta}\right)\frac{k_{eff} - k_f}{2k_{eff} + k_f} + \frac{\phi_p}{\beta}\frac{k_{eff} - k_c}{2k_{eff} + k_c} = 0 \qquad (11)$$

where k_c is the thermal conductivity of a complex sphere, which is composed of a spherical nanoparticle of thermal conductivity k_p with radius of r and an shell of thermal conductivity k_{int} with a thickness of l,

$$k_c = k_{int} \frac{2k_{int} + k_p + 2\beta(k_p - k_{int})}{2k_{int} + k_p - \beta(k_p - k_{int})} \qquad (12)$$

where $\beta = \dfrac{r^3}{(r+l)^3}$. It is demonstrated that the theoretical results on the effective

thermal conductivity of carbon oil-nanotube nanofluid and water-Al_2O_3 nanofluid are in good agreement with the experimental data. Furthermore, they interpreted the anomalous enhancement of the effective thermal conductivity of carbon oil-nanotube nanofluid and its nonlinearity with carbon nanotube loadings using Eq. (10).

It is found that the Brownian motion of nanoparticles at the molecular and

nanoscale level is a key mechanism that governs the thermal behavior of nanofluids [41]. The following context presents the second term k_c in Eq. (6) based on fractal theory [57, 82]. The heat transfer coefficient is defined as:

$$h = \frac{Nu \cdot k_f}{\lambda} \tag{13}$$

where Nu is Nusselt number for liquid flowing around a sphere, and $Nu = 2.0 + 0.5\,\mathrm{Re}\cdot\mathrm{Pr} + O(\mathrm{Re}^2 \cdot \mathrm{Pr}^2)$ [83], in which Pr is the Prandtl number of fluids and Re is the Reynolds number. Nu is related to thermal diffusion coefficient, kinematical viscosity, absolute viscosity, density and specific heat of fluid, as well as the diameter and velocity of particle. Thus, the heat transferred by convection q_λ for a single nanoparticle moving in liquids is calculated by:

$$q_\lambda = ha_\lambda \left(T_p - T_f\right) \tag{14}$$

where T_p and T_f are the temperatures of particle and liquid, respectively, a_λ is the surface area of a particle with diameter is λ.

Considering the fractal distribution of nanoparticles in nanofluids and the assumption of local thermal equilibrium, the heat transferred by convection of all particles q_c is given as [57]

$$q_c = -\int_{\lambda_{\min}}^{\lambda_{\max}} q_\lambda dN = -\int_{\lambda_{\min}}^{\lambda_{\max}} a_\lambda h \delta_T \frac{\Delta T}{\delta_T} dN \tag{15}$$

where δ_T is the thickness of the thermal boundary layer of heat convection caused by the nanoparticles' Brownian motion and $\Delta T = T_p - T_f$. By postulating that the nanolayer of the ordered liquid molecules act as a hydrodynamic boundary layer, and that three layers exist at the interface, the hydrodynamic boundary layer δ is given as $\delta = 3d_f$ and $\delta_T = \delta/\mathrm{Pr}$ (d_f is the diameter of the base liquid molecule) [41, 77].

The equivalent thermal conductivity contributed by heat convection can be

9

calculated by [57]:

$$k_c = -\frac{q_c}{A}\frac{\delta_T}{\Delta T} = \frac{1}{A}\int_{\lambda_{\min}}^{\lambda_{\max}} a_\lambda h\delta_T dN \tag{16}$$

where $A = \int_{\lambda_{\min}}^{\lambda_{\max}} \pi\lambda^2 dN$ is the total area of nanoparticles. The dimensionless expression

of k_c is

$$k_c^+ = \frac{k_c}{k_f} = \frac{1}{k_f A}\int_{\lambda_{\min}}^{\lambda_{\max}} ha_\lambda \delta_T dN \tag{17}$$

Combing Eqs. (14) and (2) with Eq. (17), we can obtain the fractal model for the dimensionless thermal conductivity caused by heat convection due to Brownian motion as [57]:

$$k_c^+ = c\frac{Nu \cdot d_f}{\Pr}\cdot\frac{2-D}{1-D}\cdot\frac{\lambda_{\max}^{1-D} - \lambda_{\min}^{1-D}}{\lambda_{\max}^{2-D} - \lambda_{\min}^{2-D}} \tag{18}$$

where c is an empirical constant, which is related to the thickness of the thermal boundary layer ($\delta_T = \delta/\Pr$). In other word, c is primarily related to the property of the host liquid, and is independent of particles [57]. The Nusselt number is taken to be 2.0 [57]. Further considering the fractals relationship of particle size distribution to fractal dimension (Eqs. (5)), Eq. (18) can be rewritten as [57]:

$$k_c^+ = c\frac{N_u \cdot d_f}{\Pr}\frac{D(2-D)}{(1-D)^2 \lambda_{av}}\frac{[\xi^{D-1}-1]^2}{\xi^{D-2}-1} \tag{19}$$

From Eq. (19), thermal conductivity caused by heat convection due to Brownian motion is a function of fluid property, temperature, average nanoparticle size, minimum and maximum nanoparticle sizes and fractal dimension, and it especially shows that it is inversely proportional to λ_{av}.

Thus, the total dimensionless effective thermal conductivity of nanofluids is obtained [57]

$$1 \quad \frac{k_{eff}}{k_f} = k_s^+ + k_c^+ = \frac{k_p + 2k_f - 2\phi_p\left(k_f - k_p\right)}{k_p + 2k_f + \phi_p\left(k_f - k_p\right)} + c\frac{N_u \cdot d_f}{\mathrm{Pr}} \frac{D(2-D)}{(1-D)^2 \lambda_{av}} \frac{\left[\xi^{D-1}-1\right]^2}{\xi^{D-2}-1} \qquad (20)$$

2 where $k_s^+ = k_s/k_f$. From Eq. (20), the total dimensionless effective thermal

3 conductivity varies with the Prandtl number, the molecule diameter of fluids, the

4 volume fraction of nanoparticles, fractal dimension and sizes of nanoparticles. Since

5 $\xi = 10^{-3}$ is assigned from above analysis, once the ϕ_p is measured, the D can be

6 calculated by Eq. (4), the thermal conductivity is then predicted from Eq. (20) as long

7 as the parameters Pr, d_f , k_f and k_p are known. From Eq. (20), it can be seen that the

8 analytical model for effective thermal conductivity of nanofluids is derived while taking

9 into account the effect of heat convection caused by Brownian motion of nanoparticle

10 based on the fractal geometry theory. The fractal model contains less empirical

11 constants, which are normally required in classical approach, and every parameter in

12 Eq. (20) has clear physical meaning. Besides the analytical method, the present fractal

13 technique might have the potential in the analysis of other transport properties such as

14 optical and electrical properties of nanofluids. So, the proposed fractal technique may

15 provide us with a new approach in addition to the analytical and other numerical

16 methods.

17 As shown in Fig. 1, the predictions made by the effective thermal conductivity

18 formulation, Eq. (20), estimate the experimental data of nanofluids well [57] (water

19 and ethylene glycol (EG) are host liquids respectively with Al_2O_3 and CuO suspensions

20 [13, 24-26, 84]). The effects of particle volume fraction and particle diameter on

21 thermal conductivity are also demonstrated in Fig. 1. The thermal conductivity

22 increases with the increasing of particle volume fraction and temperature, and decreases

23 with particle diameter. Figure 2 presents the contribution weight of convection to the

24 total thermal conductivity versus volume fraction and diameter of nanoparticles [57].

11

Clearly, there is a critical particle volume fraction (ϕ_p =0.126) for the maximum contribution from convection for different particle size. However in other works, the critical volume fraction is independent of particle diameter. This is very important for designing and preparing industrial applications liquids of high thermal conductivity.

Particles in nanofluids may randomly aggregate with each other to form various shape structures, and this has been confirmed experimentally [85]. Because chain structures allow more heat to transport than other shape structures along the direction of heat flux, the heat conduction could be enhanced due to the particle aggregation of chain shape [53]. Recently, Wei et al.[86] discussed the influence of random aggregation shape of nanoparticles for the effective thermal conductivity and modified the empirical shape factor F (proposed by Hamilton and Crosser [85] to improve Maxwell equation [87]) based on fractal theory, the F is expressed as[86]:

$$F = \frac{3D}{D-1}\frac{3-D}{2-D}\frac{\phi_p}{1-\phi_p}\left(\phi_p^{\frac{D-2}{3-D}}-1\right) \qquad (21)$$

In Hamilton and Crosser's model [85], F is constant for same shape particles (F=6 for ellipse and F=3 for sphere). However, it is observed (Eq. (21)) that F is a function of fractal dimension and concentration, and F increases with the increasing of particle concentration. Wei et al.[86] claimed that the shape of aggregation gradually grows to chain with the increasing concentration when considering the fractal distribution of nanoparticle aggregation. However, most aggregation shapes are circles when F<6.

3. Fractal and Monte Carlo simulation on convective heat transfer of nanofluids

3.1 Formulation of Convective Heat Transfer model

Figure 3 shows Al_2O_3 nanoparticles dispersed in distilled water, in which the

particles are spheres with an average diameter of 47 nm in a range from 10 nm to 100 nm, as evaluated from Transmission Electron Microscopy (TEM) images [88]. The number of nanoparticles is very large in nanofluids, and their sizes are different.

It is demonstrated that the existence of nanoparticles enhances the single-phase convection heat transfer since the nanoparticles moving in fluids carry energy and the heat exchange may occur between hot and cold regions [75, 89]. Recently, Xiao et al. [90] developed a model for the total heat flux q_t from the convective heat transfer of nanofluids (CHTNs)

$$q_t = \left[\frac{k_f}{\sum\limits_{i=1}^{J} \lambda_i^2} \sum\limits_{i=1}^{J} \lambda_i \left(2 + \frac{3}{2\alpha} \sqrt{\frac{2k_B T}{\pi \rho_p \lambda_i}} \right) + h_c \right] \Delta T \qquad (22)$$

where $k_B = 1.38 \times 10^{-23} J/K$ is the Boltzmann constant, ρ_p is the density of nanoparticle, and λ_i is the diameter of nanoparticle, and h_c is the average heat transfer coefficient by natural convection from the base fluids. The first term of the right side of Eq. (22) indicates the heat transferred by heat convection caused by Brownian motion of nanoparticles, and the second term indicates the contribution by natural convection from the base fluids. The h_c can be given by [91]

$$h_c = \begin{cases} 0.14 \rho_f c_p \left[\dfrac{\gamma_1 g(T_w - T_f)\alpha^2}{\upsilon} \right]^{1/3}, & 2 \times 10^7 < Ra < 3 \times 10^{10} \\[4mm] 0.54 \rho_f c_p \left[\dfrac{\gamma_1 g(T_w - T_f)\alpha^3}{\sqrt{A_h}\upsilon} \right]^{1/4}, & 10^5 < Ra < 2 \times 10^7 \end{cases} \qquad (23)$$

where A_h is the area of heating surface, α is thermal diffusivity of fluid, υ is kinematic viscosity, Ra is Rayleigh number, ρ_f is the base fluids density, c_p is specific heat at constant pressure, γ_1 is volumetric thermal expansion coefficient of

1   liquid, g is the gravity acceleration, T_w is wall temperature.

2   Equation (22) takes account of the effect of convection caused by the Brownian

3   motion, and relates the total heat flux from CHTNs to the parameters of nanofluid, such

4   as the nanoparticles sizes, the thermal conductivities of base fluids, and the wall

5   superheat as well as fluid properties. In Eq. (22) ΔT is a variable. When a pure liquid

6   was boiled over heating surfaces, there is a significant effect of surface characteristics

7   on boiling performance and mechanisms [92, 93]. Actually, the transport properties of

8   the heater affect the extent of the thermal interaction among the cavities, causing

9   activation and deactivation of individual cavities.

10 *3.2 Methodology for the fractal-Monte Carlo Technique*

11   The cumulative probability R (0~1) in the range of $\lambda_{min} \sim \lambda_i$ can be obtained

12 from integrating the probability density function (rewriting Eq. (3) as

13 $f(\lambda_i) = D\lambda_{min}^D \lambda_i^{-(D+1)}$) [94]

14 $$R_i(\lambda_i) = \int_{\lambda_{min}}^{\lambda_i} f(\lambda_i)d\lambda_i = \int_{\lambda_{min}}^{\lambda_i} D\lambda_{min}^D \lambda_i^{-(D+1)}d\lambda_i = 1 - \left(\frac{\lambda_{min}}{\lambda_{max}}\right)^D \qquad (24)$$

15 Eq. (24) indicates that $R = 0$ as $\lambda \to \lambda_{min}$ and $R \approx 1$ as $\lambda \to \lambda_{max}$. For the ith

16 nanoparticles chosen randomly, the diameter λ_i is expressed as[94]

17 $$\lambda_i = \frac{\lambda_{min}}{(1-R_i)^{1/D}} = \frac{\lambda_{min}}{\lambda_{max}}\frac{\lambda_{max}}{(1-R_i)^{1/D}} \qquad (25)$$

18 where $i = 1,2,3,...,J$ (J is the total number of Monte Carlo simulations in one run for a

19 given concentration). Equation (25) presents an explicit probability model for

20 nanoparticles size distribution in the present simulation, also denotes that since R_i is a

21 random number of $0 \sim 1$ produced by computer, the nanoparticle diameter λ_i is

22 determined randomly, which simulates the randomness and fractal distribution of

14

nanoparticles size.

The average diameter $\lambda_{av}^{'}$ of the all nanoparticles calculated in the presented Monte Carlo simulations can be written as [90]

$$\lambda_{av}^{'} = \frac{1}{J} \sum_{i=1}^{J} \lambda_i \qquad (26)$$

The algorithm for determination of the CHTNs is summarized as below:

i). Given a ϕ_p and λ_{av}.

ii). Find D, $\lambda_{\min}$, and $\lambda_{\max}$ from Eq. (4), respectively.

iii). Produce a random number R_i of $0 \sim 1$ by computer.

iv). Calculate λ_i from Eq. (25).

iv). If $\lambda_i > \lambda_{\max}$ or $\lambda_i < \lambda_{\min}$, return to procedure iii, otherwise continue to the next procedure.

vi). Find $\lambda_{av}^{'}$ by Eq. (26).

vii). Find the total heat flux from CHTNs q_t from Eq. (22).

Procedures iv-vii are repeated for calculation of total heat flux from CHTNs until a converged value is obtained at a given concentration. The convergence criterion is that when the following condition is satisfied, i.e.: [90]

$$\lambda_{av}^{'} = \frac{1}{J} \sum_{i=1}^{J} \lambda_i \geq \lambda_{av} \qquad (27)$$

and then stop the simulation and record the final q_t and the total number (J) in one run for a given concentration. In Eq. (27), λ_{av} is calculated from Eq. (5). If the converged heat flux from CHTNs is obtained in one run, set the heat flux from CHTNs as $q_t^{(n)}$ (n= 1, 2, 3,…, Y). Then, the average q_t is calculated by [90]

$$\langle q_t \rangle = \frac{1}{Y} \sum_{n=1}^{Y} q_t^{(n)} \tag{28}$$

where Y is the total number of runs for a given volumetric nanoparticle concentration.

The variance υ is defined as [90, 94]

$$\upsilon = \sqrt{\langle q_t^2 \rangle - \langle q_t \rangle^2} \quad , \text{ where } \quad \langle q_t^2 \rangle = \frac{1}{Y} \sum_{n=1}^{Y} q_t^{2(n)} \tag{29}$$

Above formulas presented a simple algorithm by combining the fractal geometry and Monte Carlo technique for the total heat flux from CHTNs, hereafter referred to as the FMCHT model. This model has characters of both analytical and numerical solutions, in which the characterizations of randomness and fractal distribution of nanoparticle sizes are included.

3.3 FMCHT model tests

The comparisons between the experimental results [95, 96] and FMCHT model predictions for heat flux from convective heat transfer of water-Al_2O_3 nanofluids are plotted in Fig.4a (λ_{av}=47nm and ϕ_p=1%) and in Fig. 4b (λ_{av}=38nm and ϕ_p=0.1%). It should be also noted from Fig 4 [97] that the heat flux from convective heat transfer increases with ΔT, which may be interpreted that the higher temperature may cause the stronger Brownian motion, thus may produce more contribution to the heat transfer from convection. Figure 5 shows the heat flux from convective heat transfer of CuO nanofluids versus the average diameter of nanoparticles at ϕ_p=0.2%. The heat flux at natural convection stage decreases when the nanoparticles average size increases. This can be explained by the theory of Brownian motion, smaller average size of nanoparticles in the fluids can result in higher velocity of nanoparticles' Brownian motion, and thus the heat transferred by heat convection is improved, which is

consistent with the practical physical phenomena.

The Monte Carlo technique combined with fractal geometry theory is successfully applied to predict the CHTNs, in which the convection caused by the Brownian motion and the fractal distribution of nanoparticle sizes are taken into account. The CHTNs is negatively correlated with the average size of nanoparticles but positively correlated with the wall superheat. Besides the analytical and numerical methods, the above referred techniques also have the potential in the analysis of the transport properties such as magnetic and electrical properties of nanofluids.

4. Fractal modeling for critical heat flux of nanofluids

4.1 Fractal Model

The critical heat flux (CHF) of nucleate pool boiling heat transfer in Al_2O_3 nanofluids is pictured in Fig.6 [98]. For the base fluids, it is generally recognized that the main mechanism contributing to nucleate boiling heat transfer is the bubble generation and departure from the active cavity on the superheated surface in CHF region. Thus there are two main mechanisms contributing to nucleate pool boiling heat transfer of nanofluids in the CHF region: one is the heat $q_{t,c}$ transferred by the heat convection caused by the Brownian motion of nanoparticles, and the other is the heat $q_{b,c}$ transferred by the bubbles generation and departure from the base fluids in the CHF region. In the CHF region, the total heat flux q_t of nucleate pool boiling heat transfer of nanofluids can be expressed as [97]

$$q_t = q_{t,c} + q_{b,c} \tag{30}$$

in which the $q_{t,c}$ is calculated by

1 $$q_{t,c} = \frac{D^{0.25}(4-2D)k_f[k_p(1+2\phi_p)+2k_f(1-\phi_p)](\xi^{1-D}-1)\Delta T}{(D-1)(4-D)^{0.25}[k_p(1-\phi_p)+k_f(2+\phi_p)](1-\xi^{2-D})\lambda_{av}}$$ (31)

2 The small diameter of nanoparticle may cause the increase of the velocity of

3 nanoparticle, leading to more heat transferred by nanoparticles moving in nanofluids,

4 as expressed in Eq. (31) that $q_{t,c} \propto 1/\lambda_{av}$.

5   The distribution of available cavities on the heater surface and the liquid-solid

6 contact angle determines which cavities could potentially be active. At the same time,

7 the transport properties of the heater affect the extent of the thermal interaction among

8 the cavities, causing activation and deactivation of individual cavities. Concluding, the

9 surface characteristics affect the pool boiling performance and mechanisms when a pure

10 liquid is boiled over heating surfaces. The density of active sites on the heater surface

11 is affected by the interaction among several parameters on the heater and the liquid

12 sides, as well as the liquid-solid contact angle [92, 93, 99-107].

13   The $q_{b,c}$ in Eq. (30) can be expressed as[93]

14 $$q_{b,C} = \frac{c_q D_a}{D_a+2}\frac{4\pi\alpha}{3d_{c,\max}}\left(\frac{\Delta T}{T_w-T_f}\right)^2\left(\frac{d_{c,\max}}{d_{c,\min}}\right)^{D_a+2}$$ (32)

15 where $c_q = \pi h_{fg}\rho_g\lambda_b^3/6$ is the heat flux removed by a single bubble, h_{fg} is the latent

16 heat of vaporization, ρ_g is the vapor density, $\Delta T = T_w - T_s$, T_s is the saturation

17 temperature of liquids, λ_b is the bubble departure diameter, $d_{c,\max}$ and $d_{c,\min}$ are

18 respectively the maximum and the minimum diameters of active cavity, and D_a is the

19 fractal dimension of active cavity on the heated surface.

20   Equation (23) is the fractal analytical expressions of CHF for pool boiling heat

21 transfer in nanofluids, hereafter referred to as the FACHF model, and it indicates that

22 the CHF of pool boiling heat transfer in nanofluids is explicitly related to the average

23 diameter of nanoparticles, the volumetric nanoparticle concentration, the thermal

conductivity of nanoparticles, the fractal dimensions of nanoparticles and active cavity

on the heated surface, the temperature, and the properties of fluids.

4.2 FACHF model tests

The required parameters in Eq. (30) can be found from **Appendix**. The fractal

dimension for active cavities on the heated surfaces is in the range of $1 < D_a < 2$ in

two dimensions, and increases with wall superheat. The CHF of pool boiling heat

transfer predicted by FACHF model are compared to experiments with different

nanofluids versus ΔT as shown in Fig. 7 [108, 109].

For the thermal heated disk heater under saturated temperature and atmospheric

pressure, Kim et al. [108] studied the CHF characteristics of pool boiling for TiO_2

nanofluids with λ_{av} =45 nm, ϕ_p =0.1% and Al_2O_3 nanofluids with λ_{av} =47 nm, ϕ_p

=0.1%. Besides that, the CHF of SiO_2 nanofluids in pool boiling was investigated at

λ_{av} =35 nm and ϕ_p =0.5% under atmospheric pressure [109]. The calculated CHF of

nanofluids using the introduced fractal methods was shown to a good agreement with

the available experimental results reported in the literature.

By considering of nanoparticles moving in liquids, analytical expressions for pool

boiling heat transfer of nanofluids in the CHF region based on the fractal geometry can

be derived, which can reveal the mechanism of pool boiling heat transfer on CHF in

nanofluids.

5. Fractal Model for subcooled pool boiling of nanofluids

In general, there are two main mechanisms contribute to subcooled pool boiling

heat transfer of nanofluids: the heat flux ($q_{t,c}$) from all nanoparticles moving in liquid

1   and the other ($q_{s,b}$) from subcooled pool boiling of the base fluids, respectively. Xiao

2   et al [110] derived a fractal analytical heat flux model for subcooled pool boiling of

3   nanofluids as

4    $$q_t = q_{t,c} + q_{s,b} \tag{33}$$

5   where

6

7    $$q_{t,c} = \left\{ \frac{3}{\alpha} \sqrt{\frac{2k_B T}{\pi \rho_p \lambda_{av}}} \frac{\xi^{\gamma-1.5}-1}{3-2\gamma} \left[\frac{\xi(2-\gamma)(1-\xi^{1-\gamma})}{1-\gamma} \right]^{3/2} + \frac{2\xi(2-\gamma)(\xi^{\gamma-1}+\xi^{1-\gamma}-2)}{(1-\gamma)^2} \right\} \frac{k_f \gamma \cdot \Delta T}{(1-\xi^\gamma)\lambda_{av}}$$

8    $$\tag{34}$$

9    $$q_{s,b} = \frac{\pi^2 \alpha c_p \rho_f \rho_g h_{fg}}{12 g(\rho_f - \rho_g)T_s} \frac{D_a \gamma^{-d_{fc}}}{D_a + 1} \frac{(\Delta T)^3}{\Delta T + \Delta T_{sub}} \tag{35}$$

10   In Eq. (34), $\gamma = \log_\xi^{\phi_p}$ is used for simplification. Eq. (35) indicates that the heat flux

11   of subcooled pool boiling heat transfer in nanofluids is explicitly related to the

12   nanoparticle concentration (ϕ_p), the average diameter of nanoparticles (λ_{av}), the

13   fractal dimension (D_a) of active cavity on the heated surfaces, the wall superheat (ΔT)

14   and the subcooling of fluids (ΔT_{sub}).

15   Zhou [111] investigated experimentally heat transfer characteristics of $CaCO_3$ and

16   Cu nanofluids with and without acoustic cavitation, and discussed the effects of such

17   factors as acoustical parameters, nanoparticle concentration and fluids subcooling on

18   heat transfer enhancement around a heated horizontal copper tube. Their experimental

19   results are used to test the fractal analytical model (Eq.(33)). As shown in Fig.8, there

20   are obvious deviations between theoretical and experimental data spotted at large ΔT.

21   This circumstance probably be resulted from experiment error and/or the uncertainty of

22   the parameters that has been used in the theoretical calculation of heat transfer.

6. Fractal Aggregation of nanoparticles

Nanoparticles aggregation is a time dependent dynamic process [19, 112-114]. The structure of aggregation changes continuously because of the Brownian motion. Initially (time t=0), the particles is dispersed, and then particles agglomerate so that form multiple aggregates. These individual aggregates could be treated as a new *particles* with an effective radius R_a and can thus enhance the thermal conductivity of nanofluids. Due to the aggregations, there is a maximum thermal conductivity for well-dispersed aggregates at somewhere between the two extremes, no aggregation (t =0) and complete aggregation ($t \rightarrow \infty$) [115].

The cluster structures formed by the aggregation of gold colloids, silica-colloid, coagulated aerosols or soot exhibits scale-invariance and which can be well described as fractals [60, 116-121]. Weitz and Oliveria [117] utilized transmission-electron micrographs to study the structure formed by the irreversible kinetic aggregation of uniformly sized aqueous gold colloids, and found that the structures were highly ramified and exhibited a scale invariance with fractal dimension 1.75 (see Fig. 9), which is in good consistent with simulated value of diffusion-limited aggregation when the clusters themselves are allowed to aggregate. Gharagozloo and Goodson [122] utilized static light scattering to measure the fractal dimension of aggregates formed in nanofluids over time at various temperatures and concentrations, and found that aggregates formed more quickly at higher concentrations and temperatures.

The number of particles in an aggregate N is related to the gyration aggregate radius R_a and single particle radius r_p by [123]

$$N = \left(\frac{R_a}{r_p} \right)^{D_c} = 1 + \frac{t}{t_p} \tag{36}$$

where t_p is the aggregation time constant, D_c is the fractal dimension of the aggregate, $1 \le D_c \le 3$ ($D_c = 3$ is the limit of a completely compact spherical aggregate). Available studies indicate that the D_c ranges from 1.75 to 2.5 [115]. The reaction limited particle-cluster or diffusion limited cluster-cluster aggregation (DLCCA) mode can be distinguished by the fractal dimension D_c. Irreversible particle-cluster aggregation leads to a denser aggregate than cluster-cluster aggregation with fractal dimensions of 2.5 and 1.8, respectively [123]. Waite et al.[124] found the D_c ranged from 1.8 to 2.3 for aggregation of Al_2O_3. Wang et al. [28] found that aggregation is DLCCA (D_c close to 1.8) in nanofluid. Gharagozloo and Goodson [122] found that the permanent aggregates in the nanofluid have a fractal dimension of 2.4 and the aggregate formations that grow over time are found to have a fractal dimension of 1.8, which is consistent with diffusion limited aggregation. $D_c = 1.8$ is assumed in model calculations by Prasher et al.[115].

The total mass (m_a) of particles in a single aggregate is expressed as[115]:

$$m_a = m_p \left(1 + \frac{t}{t_p} \right) \tag{37}$$

where m_p is the particle mass for a well-dispersed system.

The aggregation time constant t_p is calculated by [123]

$$t_p = \frac{\pi \mu r_p^3 W}{k_B T \phi_p} \tag{38}$$

where W (≥ 1) is the stability ratio, ϕ_p is the volume fraction of the primary particles.

From Eq. (38), t_p increases rapidly with the increasing of r_p, which means rapider

aggregation can take place for smaller particles. $t_p \rightarrow \infty$ means the system is stable and nanoparticles are well dispersed. When repulsive force and hydrodynamic interactions between the nanoparticles are absented, $W=1$, otherwise, $W > 1$ [115].

The thermal conductivity of nanofluids can be significantly enhanced by the aggregation of nanoparticles into clusters [125]. Considering that the conductivity of aggregates is based on the Bruggeman model [28], the conductivity of an aggregate (k_a) is [115]:

$$(1-\phi_{in})\frac{(k_f - k_a)}{k_f + 2k_a} + \phi_{in}\frac{k_p - k_a}{k_f + 2k_a} = 0 \tag{39}$$

where ϕ_{in} is the volume fraction of particles in aggregates, it is calculated by [126]:

$$\phi_{in} = \left(\frac{R_a}{r_p}\right)^{D_c - 3} = \left(1 + \frac{t}{t_p}\right)^{\frac{D_c - 3}{D_c}} \tag{40}$$

in Eq. (40), the maximum value $\phi_{in} = 1$ and the minimum value $\phi_{in} = \phi_p$ (see Fig. 10) [115]. The contribution due to conduction for the aggregated system can be calculated by MG model, thus rewritting Eq. (7) by instead of ϕ_p by ϕ_a, yeilds [115, 127] :

$$\frac{k_s}{k_f} = \frac{k_a + 2k_f - 2\phi_a(k_f - k_p)}{k_a + 2k_f + \phi_a(k_f - k_p)} \tag{41}$$

where $\phi_p = \phi_{in}\phi_a$. Eq. (41) is a fractal thermal conductivity model of nanofluids which combines the micro-convective effect due to Brownian motion with the change of conduction caused by particles aggregation. And it has been valided experimentally using data of nanofluids made from different sizes of nanoparticles. In developing Eq. (41), nanoparticles are assumed to be spherical and of uniform size, and effects of thermal

boundary resistance between particles and fluid are neglected. For well dispersed system, $\phi_{in} = 1$ and $\phi_p = \phi_a$, Eq. (41) reduces to the MG model (see Eq. (7)) [115].

Figure 10 shows the comparison between the model predictions for aggregated nanoparticles (Eq. (41)) and well dispersed nanoparticles (Eq. (7)). As shown in this figure, the enhancement due to particle aggregation is well demonstrated compared with that for a well-dispersed system. For the percolation effects in the agglomerate, the limiting value ($\phi_{in} = \phi_p$) is slightly higher than that in the MG model. Obviously, particle aggregation enhances the conduction contribution when the aggregates are well dispersed and none large aggregate is formed [115].

Following above mentioned works on the effects of aggregation and its kinetics on thermal conductivity [28, 115], Prasher et al [125] further developed a three-level homogenization theory to evaluate the effective thermal conductivity of colloids containing fractal clusters. In other aspect, Gaganpreet and Srivastava [128] theoretically studied the viscosity of oxide nanoparticle dispersions based of fractals of irregular structure of aggregation, and they used prolate ellipsoid aggregation to study the viscosity of nanofluids.

Nanoparticle aggregate also shows multifractal [129, 130]. However, for the theatrical determining of the fractal dimension of nanoparticle aggregates, the available methods usually under the limitation of the finite scale/range of self-similarity of physical objects and the resolution of scanning electron microscope (SEM) and TEM methods [131]. Recently, Wozniak et al. [132] also found that multi-scale analysis of a large sample is not suitable to derive morphological parameter of multi-fractal samples of particle aggregates. They further introduced the modified Box-Counting (MBC) algorithm to estimate the fractal dimension of each aggregate from its own self-

similarity properties. MBC validity was tested successfully on synthetic aggregates whose fractal dimension was independent of or correlated with aggregate size.

7. Fractal analysis on yield stress property of nanoparticle aggregation

Besides the attentions on enhancement thermal conductivity of nanoparticles and its cluster in nanofluids, other physical behaviours of the nanoparticle aggregation system also received many attentions, e.g., its yield stress property. It is well accepted that the expression of yield stress μ is a power function of the solid volume fraction [118, 121, 133]:

$$\mu = \mu_0 \phi_a^m \tag{42}$$

where μ_0 is the referenced parameter ($\mu = \mu_0$ at $\phi_a = 1$), ϕ_a is the solid volume fraction, m is a constant, which is set as different values by different researchers through capturing the role of the aggregate size and the solid volume fraction on yield stress, leaving the number of fitting parameters to a minimum [133]. Combining the fractal model for the aggregate backbones and the aggregate volume, Xi et al. [133] developed a fractal model for the yield stress of aggregates by taking the solid volume fraction and the aggregate diameter into consideration. In Xi et al.'s model [133], the constant m is expressed as:

$$m = \frac{2X - 3D_c}{3(D_c - 3)} \tag{43}$$

where X is the backbone fractal dimension, which is less than the fractal dimension of the aggregate D_c and is larger than unity to provide a connected path. In Eq. (43), D_c can be determined using small angle X-ray scattering (SAXS), but X is not clearly stated

25

in literatures.

Eq. (43) is more generalized compared to other available models. If $X=D_c$, Eq. (43) reduces to the model by Xu et al.[134]:

$$m = \frac{D_c}{3(3-D_c)} \tag{44}$$

and if $X = 5D_c/2 - 3$, the exponent $m=2/3$ from Eq. (43), which is the same as the result of Son and Hsu[135]. Based on Mandelbrot's rules of thumb [60] and analysis of experimental results, Xi et al[133] argued that the relation $X = D_c - 1$ can be as a simple method to evaluate the backbone fractal dimension.

By introducing the novel express of constant, the model, Eq. (42), can fit experimental data for polymer system [136] and silica aerogel system well [137], as shown in Fig. 12 [133]. The fractal dimension $D_c = 2.4$ is respectively measured by SAXS method. The SAXS experiments are briefly presented here. A beam of light is directed onto the sample and the scattered light intensity $I(Q)$ is measured as a function of the magnitude of the scattering vector Q, the scaling law between them can be expressed as [138]:

$$I(Q) \sim Q^{-D_c} \tag{45}$$

From Eq. (45), the fractal dimension D_c can be determined by the value of the slope of a linear fit through data on a logarithmic plot of $I(Q)$ versus Q in the range of $1/R_a < Q < 1/r_p$.

8. Discussion and Future Work

Although fractal-based approaches have been proposed to study the heat transfer of nanofluids and the aggregation process of nanoparticles as well as the yield stress

26

property of nanoparticles aggregation, a gap still exists between the expected fruits and presented status. Generally, comparing with other mathematical models, fractal methods expressed the thermal conductivity analytically. What's more less empirical constants are included in the fractal models, which are normally required in other mathematical models. In addition to these advantages, the fractal technique might be potentially applied in analyzing of other transport properties such as optical and electrical properties of nanofluids. So, the fractal technique provides us a new approach besides other numerical methods. However, the shortcoming of fractal theory for application in nanofluids and nanoparticle aggregation is that it should be noticed that it only works fair when $\zeta \leq 10^{-2}$. For nanofluid and nanoparticle aggregation $\zeta \leq 10^{-2}$, so the fractal theory can be used to analyze the characters of nanofluids and nanoparticle aggregation.

Further research directions and subjects concerning the transport and other properties of nanoparticle system may be anticipated in:

(a) The nanoparticle aggregation is a kinetic process, which is verified to be characterized well by fractal model [115] and be consistent with the diffusion limited aggregation [122]. Thus, the fractal and multi-fractal theories [139, 140] combined with diffusion limited aggregation model can be used to simulate the nanoparticle aggregation and its influence on the heat transfer of nanofluids.

(b) From the theoretical equation for predicting fractal dimension (Eq. (4)), the necessary values for the volume fraction and the minimum and maximum size of nanoparticle aggregation needed to be measured by other experimental methods (Such as SEM and TEM). However, in the process of aggregation of nanoparticles, fractal dimension of aggregates is a time dependent variable. How would the fractal dimension change over time at various temperatures need to be further analysed.

Static light scattering has been used to obtain the average fractal dimension of aggregation of nanoparticles over time at different length-scales and temperatures [122]. By utilizing Static light scattering technology, the effect of dynamic aggregation process of nanoparticle on heat transfer of nanofluids can be analysed.

(c) Generally, the particles are not spherical and smooth, the shape and surface roughness influence the contact area, and further influence the heat transfer between particles and particles, also between the particles and host liquid [141]. The fractal theory can be used to characterize the surface roughness [142, 143] and analyse its influence on the heat transfer of nanofluids and the yield stress property of nanoparticle aggregation.

(d) Nanoparticle aggregation in nanofluids is a bi-dispersed porous medium, multiscale phenomenon and its effect also needed to be further analysed. Besides the pore mass fractal model, the solid mass fractal model as well as the pore-solid fractal model [144-146] may also be potential approach to nanofluids and nanoparticle aggregation.

(e) Nanoparticle aggregates in the gas phase is demonstrated to be multifractal [129]. We argue that this conclusion also apply to nanoparticle in liquid. Thus, how the strength and conductivity properties of these multifractal aggregates influenced by the interaction between the different scales needs to be attended.

(f) For the particle aggregates influence the properties of nanofluids, is it possible to design arithmetic with prospective fractal structures to optimize the heat transfer of nanofluids, which is an interesting direction and a challenging issue in nanoscience.

(g) Nanoparticle clusters is mixed dynamic behaviour, in which fractal is one of key characterizations. In other word, whole phenomenon of kinetics aggregation can't be fully explained only by one approach. It is necessity to combine other theory or method, such as effective medium theory, percolation theory [147], which would

be applied to analyse properties of nanofluids. Remarkable, fractal theory has been one of the basic methods for kinetics aggregation of nanofluids.

(h) Besides the combining of fractal theory and Monte Carlo technique [94, 148], the fractal-based method may also be incorporated in other numerical simulation technique in future, such as molecular dynamics simulation, lattice Boltzmann methods, and other computational fluid dynamics methods.

(i) The dye diffusion in nanofluids is analogous to heat transfer in nanofluids and has been taken as a strong evidence for the role of micro convection by Brownian motion of particles, the enhanced mass transport visualized could be due to the stabilizer effect as the introduced surfactant could significantly reduce viscosity [149]. Therefore, whether the thermal conductivity enhancement is caused by Brownian motion particles or the reduced viscosity due to the surfactant still need to be further discussed.

9. Conclusions

Nanofluids, consisting of suspended nanoparticles and base liquids, usually have much higher thermal conductivity than the pure base liquids even at very small volume fractions of nanoparticles. Nanoparticles aggregation is a time dependent phenomenon, and can form continuously complex structure system because of the Brownian motion. It has been shown experimentally and numerically that nanoparticles and its aggregation can be well described by fractal theory.

This review briefly reviewed the advances of nanoparticles researches and introduced the fractal theory. Then, presented the fractal model of thermal conductivity of nanofluids by taking into account the fractal distribution of nanoparticle sizes and heat convection between nanoparticles and liquids due to the Brownian motion of nanoparticles in fluids, in which the nanoparticles is assumed to be dispersed.

With the consideration of nanoparticles moving fluids, three novel fractal models for heat transfer of nanofluids including convective heat transfer, critical heat flux and subcooled pool boiling heat transfer were introduced. Besides, three formulas of predicting the heat flux of boiling heat transfer was summarized, in which the discussed fractal models were in terms of the average diameter of nanoparticles, the volumetric nanoparticle concentration, the thermal conductivity of nanoparticle, the fractal dimensions of nanoparticles and active cavity on the heated surface, the temperature, the wall superheat, the subcooling of fluids, and the properties of fluids. An excellent agreement between the fractal model predictions and experimental data was found.

By considering the fractal property of particle aggregate, we also further analyzed the contribution thermal conductivity due to conduction for the aggregated system developed from MG model. At last, the yield stress property of nanoparticle aggregation was fractal summarized.

Appendix

The bubble departure diameter λ_b can be obtained as [150]

$$\lambda_b = c_0 \left[\frac{\sigma}{g(\rho_f - \rho_g)} \right]^{1/2} Ja^{*5/4} \tag{A1}$$

with $c_0 = 1.5 \times 10^{-4}$ for water, and $c_0 = 4.65 \times 10^{-4}$ for the other liquid, σ is the surface tension of liquid, Ja^* is the Jakob number which is given by

$$Ja^* = \frac{\rho_l c_{pl} T_s}{\rho_g h_{fg}} \tag{A2}$$

The minimum and the maximum active cavity diameter ($d_{c,\min}$ and $d_{c,\max}$) can be predicted by the model as [151]

$$d_{c,\min} = \frac{2\delta}{C_1}\left[1 - \frac{\theta_s}{\theta_w} - \sqrt{\left(1 - \frac{\theta_s}{\theta_w}\right)^2 - \frac{4\zeta_1 C_2}{\delta\theta_w}}\right] \tag{A3}$$

$$d_{c,\max} = \frac{2\delta}{C_1}\left[1 - \frac{\theta_s}{\theta_w} + \sqrt{\left(1 - \frac{\theta_s}{\theta_w}\right)^2 - \frac{4\zeta_1 C_2}{\delta\theta_w}}\right] \tag{A4}$$

where $\zeta_1 = 2\sigma T_s/(\rho_g h_{fg})$; $C_1 = (1+\cos\theta)/\sin\theta$ and $C_2 = 1+\cos\theta$, with θ being

the contact angle of the fluid and the heater material; $\theta_s = T_s - T_f$; $\theta_w = T_w - T_f$; and

δ is the thermal boundary layer thickness in nanofluid which can be expressed as

$$\delta = \frac{k_{eff}}{h} \tag{A5}$$

In nucleate pool boiling of the base fluids, the fractal dimension of active cavity

D_a on the heated surface is given by [99]

$$D_a = 2\frac{\ln\sqrt{2}d_{c,\min} - \ln\overline{d}_{c,\max}}{\ln\gamma} \tag{A6}$$

where $\gamma = d_{c,\min}/d_{c,\max}$. Here $\overline{d}_{c,\max}$ is the averaged value over all the maximum

active cavities

$$\overline{d}_{c,\max} = \frac{1}{T_w - T_s}\int_{T_s}^{T_w} d_{c,\max}T_w dT_w = \frac{1}{\Delta T}\sum_{j=1}^{N} d_{c,\max}T_{w_j}\delta T_w = \frac{1}{N}\sum_{j=1}^{N} d_{c,\max}T_{w_j} \tag{A7}$$

where $N = \Delta T/\delta T_w$, and δT_w is assumed to be a constant. In the above equation,

$T_{w_j} = T_s + j(\delta T_w)$ with j=1, 2,…, N. For example, if we choose $\delta T_w = 0.2°C$ then

N=5 for $\Delta T = 1°C$, and N=50 for $\Delta T = 10°C$.

Nomenclature

A total area of nanoparticles

c empirical constant in Eq. (18)

c_p specific heat at constant pressure

1. D fractal dimension of nanoparticle

2. D_a fractal dimension of active cavity

3. D_c fractal dimension of the aggregate

4. $d_{c,\max}$ maximum diameters of active cavity

5. $d_{c,\min}$ minimum diameters of active cavity

6. d_E Euclidean dimension

7. d_f diameter of base liquid molecule

8. g gravity acceleration,

9. h heat transfer coefficient

10. I scattered light intensity

11. Ja^* Jakob number

12. k thermal conductivity

13. k_B Boltzmann constant

14. M mass of a fractal object

15. m constant in Eq. (41)

16. m_a total mass of particles aggregate

17. m_p dispersed particle mass

18. N number of particle

19. Nu Nusselt number

20.   Pr   Prandtl number

21. q heat transfer

22. Q scattering vector

23. R cumulative probability

24. R_a gyration aggregate radius

1. Ra   Rayleigh number,

2. Re   Reynolds number.

3. r_p single particle radius

4. T temperatures

5. t_p aggregation time constant

6. T_s saturation temperature of liquids

7. W stability ratio

8. X backbone fractal dimension

9. Subscripts

10. a   aggregate

11. av   average

12. c   convection

13. eff   effective

14. f   fluid

15. h   heating

16. min   minimum

17. max   maximum

18. p   particle

19. s   stationary

20. t   total

21. w   wall

22. Greek letters

23. α thermal diffusivity

24. γ_1 volumetric thermal expansion coefficient

25. δ_T thermal boundary layer thickness

1. ε measured scale

2. θ contact angle

3. λ particle size

4. μ yield stress

5. ξ dimensionless coefficient

6. ρ_p nanoparticle density

7. ρ_g vapor density,

8. σ surface tension of liquid

9. υ kinematic viscosity

10. ϕ volume fraction

11. ϕ_{in} volume fraction of particles in aggregates

Acknowledgements

References

[1]. A. C. Balazs, T. Emrick,T. P. Russell, Nanoparticle polymer composites: Where two small worlds meet. Science, 314 (2006) 1107-1110.

[2]. S. Senthilraja, M. Karthikeyan,R. Gangadevi, Nanofluid applications in future automobiles: Comprehensive review of existing data. Nano-Micro Lett., 2 (2010) 306-310.

[3]. B. I. Kharisov, O. V. Kharissova,U. Ortiz-Mendez, Crc concise encyclopedia of

nanotechnology. 2015: CRC Press.

[4]. S. Kano, T. Tada,Y. Majima, Nanoparticle characterization based on stm and sts. Chem. Soc. Rev., 44 (2015) 970-987.

[5]. A. K. Sharma, A. K. Tiwari,A. R. Dixit, Progress of nanofluid application in machining: A review. Mater. Manuf. Process., 30 (2015) 813-828.

[6]. E. Sadeghinezhad, M. Mehrali, R. Saidur, et al., A comprehensive review on graphene nanofluids: Recent research, development and applications. Energ. Convers. Manage., 111 (2016) 466-487.

[7]. S. U. S. Choi, J. A. Eastman, *Enhancing thermal conductivity of fluids with nanoparticles*, in *Development and applications of non-nemtonian flows*, Siginer, D.A. and Wang, H.P., Editors. 1995, ASME FED-vol 231/MD-vol 66 (New York: ASME). p. 99-106.

[8]. X.-Q. Wang, A. S. Mujumdar, Heat transfer characteristics of nanofluids: A review. Int. J. Thermal. Sci., 46 (2007) 1-19.

[9]. S. A. Angayarkanni, J. Philip, Review on thermal properties of nanofluids: Recent developments. Adv. Colloid Interface Sci., 225 (2015) 146-176.

[10]. J. C. Cai, Y. W. Ju, X. Y. Hu, et al., *Fractal properties of nanoparticle aggregation*, in *Advanced environmental analysis: Applications of nanomaterials, volume 1*, Hussain, C.M. and Kharisov, B., Editors. 2016, The Royal Society of Chemistry. p. 58-73.

[11]. X. Fang, Y. Chen, H. Zhang, et al., Heat transfer and critical heat flux of nanofluid boiling: A comprehensive review. Renew. Sust. Energ. Rev., 62 (2016) 924-940.

[12]. T. Bauer, A general analytical approach toward the thermal conductivity of porous media. Int. J. Heat Mass Transfer, 36 (1993) 4181-4191.

[13]. J. A. Eastman, S. U. S. Choi, S. Li, et al., Anomalously increased effective thermal conductivities of ethylene glycol-based nanofluids containing copper nanoparticles. Appl. Phys. Lett., 78 (2001) 718-720.

[14]. S. Murshed, K. Leong,C. Yang, Investigations of thermal conductivity and viscosity of nanofluids. Int. J. Thermal. Sci., 47 (2008) 560-568.

[15]. J. Eapen, R. Rusconi, R. Piazza, et al., The classical nature of thermal conduction in nanofluids. J. Heat Transfer 132 (2010) 102402.

[16]. H. Aminfar, R. Motallebzadeh,A. Farzadi, The study of the effects of thermophoretic and brownian forces on nanofluid thermal conductivity using lagrangian and eulerian approach. Nanoscale Microscale Thermophys. Eng. , 14 (2010) 187-208.

[17]. G. Okeke, S. Witharana, S. Antony, et al., Computational analysis of factors influencing thermal conductivity of nanofluids. J. Nanopart. Res., 13 (2011) 6365-6375.

[18]. J. M. Kshirsagar, R. Shrivastava, Review of the influence of nanoparticles on thermal conductivity, nucleate pool boiling and critical heat flux. Heat Mass Transfer, 51 (2015) 381-398.

[19]. P. Keblinski, J. A. Eastman,D. G. Cahill, Nanofluids for thermal transport. Mater. Today 8(2005) 36-44.

[20]. H. E. Patel, S. K. Das, T. Sundararajan, et al., Thermal conductivities of naked

and monolayer protected metal nanoparticle based nanofluids: Manifestation of anomalous enhancement and chemical effects. Appl. Phys. Lett., 83 (2003) 2931-2933.

[21]. S. A. Putnam, D. G. Cahill, P. V. Braun, et al., Thermal conductivity of nanoparticle suspensions. J. Appl. Phys., 99 (2006) 084308.

[22]. A. T. Utomo, H. Poth, P. T. Robbins, et al., Experimental and theoretical studies of thermal conductivity, viscosity and heat transfer coefficient of titania and alumina nanofluids. Int. J. Heat Mass Transfer, 55 (2012) 7772-7781.

[23]. J. Buongiorno, D. C. Venerus, N. Prabhat, et al., A benchmark study on the thermal conductivity of nanofluids. J. Appl. Phys., 106 (2009) 094312.

[24]. H. Masuda, A. Ebata, K. Teramae, et al., Alteration of thermal conductivity and viscosity of liquid by dispersing ultra-fine particles. Dispersion of al_2o_3, sio_2 and tio_2 ultra-fine particles. Netsu Bussei (Japan), 4 (1993) 227-233.

[25]. S. Lee, S. U. S. Choi, S. Li, et al., Measuring thermal conductivity of fluids containing oxide nanoparticles. J. Heat Transfer 121 (1999) 280-289.

[26]. H. Xie, J. Wang, T. Xi, et al., Thermal conductivity enhancement of suspensions containing nanosized alumina particles. J. Appl. Phys., 91 (2002) 4568-4572.

[27]. H. Xie, J. Wang, T. Xi, et al., Thermal conductivity of suspensions containing nanosized sic particles. Int. J. Thermophys., 23 (2002) 571-580.

[28]. B. X. Wang, L. P. Zhou,X. F. Peng, A fractal model for predicting the effective thermal conductivity of liquid with suspension of nanoparticles. Int. J. Heat Mass Transfer, 46 (2003) 2665-2672.

[29]. S. M. S. Murshed, K. C. Leong,C. Yang, Enhanced thermal conductivity of tio_2—water based nanofluids. Int. J. Thermal. Sci., 44 (2005) 367-373.

[30]. M. Chandrasekar, S. Suresh,A. Chandra Bose, Experimental investigations and theoretical determination of thermal conductivity and viscosity of al2o3/water nanofluid. Exp. Therm Fluid Sci., 34 (2010) 210-216.

[31]. M. J. Pastoriza-Gallego, L. Lugo, J. L. Legido, et al., Thermal conductivity and viscosity measurements of ethylene glycol-based al_2o_3 nanofluids. Nanoscale Res. Lett. , 6 (2011) 1-11.

[32]. C. Pang, J.-Y. Jung, J. W. Lee, et al., Thermal conductivity measurement of methanol-based nanofluids with al_2o_3 and sio_2 nanoparticles. Int. J. Heat Mass Transfer, 55 (2012) 5597-5602.

[33]. D. U. Mehta, R. S. Khedkar, A. S. Kiran, et al., Thermo – physical characterization of paraffin based fe_3o_4 nanofluids. Procedia Eng., 51 (2013) 342-346.

[34]. L. Syam Sundar, E. Venkata Ramana, M. K. Singh, et al., Thermal conductivity and viscosity of stabilized ethylene glycol and water mixture al2o3 nanofluids for heat transfer applications: An experimental study. Int. Commun. Heat Mass Transfer, 56 (2014) 86-95.

[35]. G. Xia, R. Liu, J. Wang, et al., The characteristics of convective heat transfer in microchannel heat sinks using al_2o_3 and tio_2 nanofluids. Int. Commun. Heat Mass Transfer, 76 (2016) 256-264.

[36]. B. A. Suleimanov, H. F. Abbasov, Effect of copper nanoparticle aggregation on the thermal conductivity of nanofluids. Russ. J. Phys. Chem. A, 90 (2016) 420-

428.

[37]. J. Fan, L. Wang, Review of heat conduction in nanofluids. J. Heat Transfer 133 (2011) 040801.

[38]. W. Daungthongsuk, S. Wongwises, A critical review of convective heat transfer of nanofluids. Renew. Sust. Energ. Rev., 11 (2007) 797-817.

[39]. D. H. Shou, J. T. Fan, M. F. Mei, et al., An analytical model for gas diffusion though nanoscale and microscale fibrous media. Microfluid. Nanofluid., 16 (2014) 381-389.

[40]. A. P. Sasmito, J. C. Kurnia, A. S. Mujumdar, Numerical evaluation of laminar heat transfer enhancement in nanofluid flow in coiled square tubes. Nanoscale Res. Lett., 6 (2011) 376.

[41]. S. P. Jang, S. U. S. Choi, Role of brownian motion in the enhanced thermal conductivity of nanofluids. Appl. Phys. Lett., 84 (2004) 4316-4318.

[42]. J. Kim, C. K. Choi, Y. T. Kang, et al., Effects of thermodiffusion and nanoparticles on convective instabilities in binary nanofluids. Nanoscale Microscale Thermophys. Eng. , 10 (2006) 29-39.

[43]. M.-S. Liu, M. C.-C. Lin, C. Tsai, et al., Enhancement of thermal conductivity with cu for nanofluids using chemical reduction method. Int. J. Heat Mass Transfer, 49 (2006) 3028-3033.

[44]. M. Chopkar, S. Sudarshan, P. Das, et al., Effect of particle size on thermal conductivity of nanofluid. Metallurg. Mater. Transact. A, 39 (2008) 1535-1542.

[45]. W. Pabst, E. Gregorová, The thermal conductivity of alumina–water nanofluids from the viewpoint of micromechanics. Microfluid. Nanofluid., 16 (2014) 19-28.

[46]. S. Hassani, R. Saidur, S. Mekhilef, et al., A new correlation for predicting the thermal conductivity of nanofluids; using dimensional analysis. Int. J. Heat Mass Transfer, 90 (2015) 121-130.

[47]. C. Pang, J. W. Lee, Y. T. Kang, Enhanced thermal conductivity of nanofluids by nanoconvection and percolation network. Heat and Mass Transfer, 52 (2016) 511-520.

[48]. P. Keblinski, S. R. Phillpot, S. U. S. Choi, et al., Mechanisms of heat flow in suspensions of nano-sized particles (nanofluids). Int. J. Heat Mass Transfer, 45 (2002) 855-863.

[49]. W. Yu, S. U. S. Choi, The role of interfacial layers in the enhanced thermal conductivity of nanofluids: A renovated maxwell model. J. Nanopart. Res., 5 (2003) 167-171.

[50]. W. Yu, S. U. S. Choi, The role of interfacial layers in the enhanced thermal conductivity of nanofluids: A renovated hamilton–crosser model. J. Nanopart. Res., 6 (2004) 355-361.

[51]. G. Huminic, A. Huminic, Heat transfer and flow characteristics of conventional fluids and nanofluids in curved tubes: A review. Renew. Sust. Energ. Rev., 58 (2016) 1327-1347.

[52]. C. Qi, L. Liang, Z. Rao, Study on the flow and heat transfer of liquid metal based nanofluid with different nanoparticle radiuses using two-phase lattice boltzmann method. Int. J. Heat Mass Transfer, 94 (2016) 316-326.

[53]. K. S. Hong, T.-K. Hong,H.-S. Yang, Thermal conductivity of fe nanofluids depending on the cluster size of nanoparticles. Appl. Phys. Lett., 88 (2006) 031901.

[54]. K. B. Anoop, T. Sundararajan,S. K. Das, Effect of particle size on the convective heat transfer in nanofluid in the developing region. Int. J. Heat Mass Transfer, 52 (2009) 2189-2195.

[55]. Y. Feng, B. Yu, K. Feng, et al., Thermal conductivity of nanofluids and size distribution of nanoparticles by monte carlo simulations. J. Nanopart. Res., 10 (2008) 1319-1328.

[56]. K. Hadjov, D. Dontchev, Influence of the particle size distribution on the thermal conductivity of nanofluids. J. Nanopart. Res., 11 (2009) 1713-1718.

[57]. J. Xu, B. M. Yu, M. Q. Zou, et al., A new model for heat conduction of nanofluids based on fractal distributions of nanoparticles. J. Phys. D. Appl. Phys., 39 (2006) 4486-4490.

[58]. S. Havlin, D. Ben-Avraham, Diffusion in disordered media. Adv. Phys., 36 (1987) 695-798.

[59]. B. Q. Xiao, Y. Yang,L. X. Chen, Developing a novel form of thermal conductivity of nanofluids with brownian motion effect by means of fractal geometry. Powder Technol., 239 (2013) 409-414.

[60]. B. B. Mandelbrot, The fractal geometry of nature. 1982, New York: W. H. Freeman.

[61]. M. Sahimi, Flow phenomena in rocks: From continuum models to fractals, percolation, cellular automata, and simulated annealing. Rev. Mod. Phys., 65 (1993) 1393-1534.

[62]. E. Perfect, Y. Pachepsky,M. A. Martin, Fractal and multifractal models applied to porous media. Vadose Zone J., 8 (2009) 174-176.

[63]. J. C. Cai, L. Luo, R. Ye, et al., Recent advances on fractal modeling of permeability for fibrous porous media. Fractals, 23 (2015) 1540006.

[64]. R. Liu, Y. Jiang, B. Li, et al., Estimating permeability of porous media based on modified hagen–poiseuille flow in tortuous capillaries with variable lengths. Microfluid. Nanofluid., 20 (2016) 120.

[65]. Z.-Y. Yang, H. R. Pourghasemi,Y.-H. Lee, Fractal analysis of rainfall-induced landslide and debris flow spread distribution in the chenyulan creek basin, taiwan. J. Earth Sci., 27 (2016) 151-159.

[66]. J. C. Cai, B. M. Yu, M. Q. Zou, et al., Fractal characterization of spontaneous co-current imbibition in porous media. Energy Fuels, 24 (2010) 1860-1867.

[67]. G. Pia, C. Esposito Corcione, R. Striani, et al., Thermal conductivity of porous stones treated with uv light-cured hybrid organic–inorganic methacrylic-based coating. Experimental and fractal modeling procedure. Prog. Org. Coat., 94 (2016) 105-115.

[68]. A. Majumdar, B. Bhushan, Role of fractal geometry in roughness characterization and contact mechanics of surfaces. J. Tribol., 112 (1990) 205-216.

[69]. B. M. Yu, P. Cheng, A fractal permeability model for bi-dispersed porous media. Int. J. Heat Mass Transfer, 45 (2002) 2983-2993.

[70]. B. M. Yu, J. H. Li, Some fractal characters of porous media. Fractals, 9 (2001) 365-372.

[71]. Y. J. Feng, B. M. Yu, M. Q. Zou, et al., A generalized fractal geometry model for the effective thermal conductivity of porous media base on self-similarity. J. Phys. D. Appl. Phys., 37 (2004) 3030-3040.

[72]. X. B. Jiang, J. K. Wang, B. H. Hou, et al., Progress in the application of fractal porous media theory to property analysis and process simulation in melt crystallization. Ind. Eng. Chem. Res., 52 (2013) 15685-15701.

[73]. W. Wei, J. C. Cai, X. Y. Hu, et al., An electrical conductivity model for fractal porous media. Geophys. Res. Lett., 42 (2015) 4833-4840.

[74]. G. Pia, U. Sanna, A geometrical fractal model for the porosity and thermal conductivity of insulating concrete. Constr. Build. Mater., 44 (2013) 551-556.

[75]. B. Q. Xiao, B. M. Yu, Z. C. Wang, et al., A fractal model for heat transfer of nanofluids by convection in a pool. Phys. Lett. A, 373 (2009) 4178-4181.

[76]. J. C. Maxwell Garnett, Colours in metal glasses and in metal films. Philos. Trans. R. Soc. London, Sect. A, 203 (1904) 385-420.

[77]. C. J. Yu, A. G. Richter, A. Datta, et al., Observation of molecular layering in thin liquid films using x-ray reflectivity. Phys. Rev. Lett., 82 (1999) 2326-2329.

[78]. T. Suzuki, D. Ohara, Intermolecular energy transfer at a solid-liquid interface. Microscale Thermophys. Eng., 4 (2000) 189-196.

[79]. S. U. S. Choi, Z. G. Zhang, W. Yu, et al., Anomalous thermal conductivity enhancement in nanotube suspensions. Appl. Phys. Lett., 79 (2001) 2252-2254.

[80]. Q.-Z. Xue, Model for effective thermal conductivity of nanofluids. Phys. Lett. A, 307 (2003) 313-317.

[81]. Q. Xue, W.-M. Xu, A model of thermal conductivity of nanofluids with interfacial shells. Mater. Chem. Phys., 90 (2005) 298-301.

[82]. V. V. Vysotskii, V. I. Roldughin,O. Y. Uryupina, Formation of fractal structures upon the evaporation of nanoparticle dispersion droplets. Colloid J., 66 (2004) 777-779.

[83]. S. Tomitika, T. Aoi,H. Yosinabu, On the forces acting on a circular cylinder set obliquely in a uniform stream at low values of reynolds number. Proc. R. Soc. London, Ser. A, 129 (1953) 233.

[84]. S. K. Das, N. Putra, P. Thiesen, et al., Temperature dependence of thermal conductivity enhancement for nanofluids. J. Heat Transfer, 125 (2003) 567-574.

[85]. R. L. Hamilton, O. K. Crosser, Thermal conductivity of heterogeneous two-component systems. Ind. Eng. Chem. Fundam., 1 (1962) 187-191.

[86]. W. Wei, J. Cai, X. Hu, et al., Fractal analysis of the effect of particle aggregation distribution on thermal conductivity of nanofluids. Phys. Lett. A, 380 (2016) 2953-2956.

[87]. J. C. Maxwell, A treatise on electricity and magnetism. 1892, London: Oxford University Press.

[88]. H. D. Kim, J. Kim,M. H. Kim, Experimental studies on chf characteristics of nano-fluids at pool boiling. Int. J. multiphase flow, 33 (2007) 691-706.

[89]. B. Q. Xiao, G. P. Jiang,L. X. Chen, A fractal study for nucleate pool boiling heat transfer of nanofluids. Sci. China-Phys. Mech. Astron., 53 (2010) 30-37.

[90]. B. Q. Xiao, G. P. Jiang, Y. Yang, et al., Prediction of convective heat transfer of nanofluids based on fractal-monte carlo simulations. Int. J. Mod. Phys. C, 24 (2013) 1250090.

[91]. C.-Y. Han, P. Griffith, The mechanism of heat transfer in nucleate pool boiling—part i. Int. J. Heat Mass Transfer, 8 (1965) 887-904.

[92]. B. Q. Xiao, B. M. Yu, A fractal model for critical heat flux in pool boiling. Int. J. Therm. Sci., 46 (2007) 426-433.

[93]. B. Q. Xiao, B. M. Yu, A fractal analysis of subcooled flow boiling heat transfer. Int. J. Multiphase Flow, 33 (2007) 1126-1139.

[94]. B. M. Yu, M. Q. Zou, Y. J. Feng, Permeability of fractal porous media by monte carlo simulations. Int. J. Heat Mass Transfer, 48 (2005) 2787-2794.

[95]. S. K. Das, N. Putra, W. Roetzel, Pool boiling characteristics of nano-fluids. Int. J. Heat Mass Transfer, 46 (2003) 851-862.

[96]. I. C. Bang, S. H. Chang, Boiling heat transfer performance and phenomena of al_2o_3–water nano-fluids from a plain surface in a pool. Int. J. Heat Mass Transfer, 48 (2005) 2407-2419.

[97]. B. Q. Xiao, Prediction of heat transfer of nanofluid on critical heat flux based on fractal geometry. Chin. Phys. B, 22 (2013) 014402.

[98]. S. Kim, I. C. Bang, J. Buongiorno, et al., Surface wettability change during pool boiling of nanofluids and its effect on critical heat flux. Int. J. Heat Mass Transfer, 50 (2007) 4105-4116.

[99]. B. Yu, P. Cheng, A fractal model for nucleate pool boiling heat transfer. ASME J. Heat Transfer, 124 (2002) 1117-1124.

[100]. G. Rosengarten, J. Cooper-White, G. Metcalfe, Experimental and analytical study of the effect of contact angle on liquid convective heat transfer in microchannels. Int. J. Heat Mass Transfer, 49 (2006) 4161-4170.

[101]. M. Prat, On the influence of pore shape, contact angle and film flows on drying of capillary porous media. Int. J. Heat Mass Transfer, 50 (2007) 1455-1468.

[102]. A. Mukherjee, S. G. Kandlikar, Numerical study of single bubbles with dynamic contact angle during nucleate pool boiling. Int. J. Heat Mass Transfer, 50 (2007) 127-138.

[103]. H. D. Kim, M. H. Kim, Effect of nanoparticle deposition on capillary wicking that influences the critical heat flux in nanofluids. Appl. Phys. Lett., 91 (2007) 014104.

[104]. Y. Sun, S. Gao, F. Lei, et al., Atomically-thin two-dimensional sheets for understanding active sites in catalysis. Chem. Soc. Rev., 44 (2015) 623-636.

[105]. K. Wan, G.-F. Long, M.-Y. Liu, et al., Nitrogen-doped ordered mesoporous carbon: Synthesis and active sites for electrocatalysis of oxygen reduction reaction. Appl. Catal., B 165 (2015) 566-571.

[106]. J. Kibsgaard, Z. Chen, B. N. Reinecke, et al., Engineering the surface structure of mos2 to preferentially expose active edge sites for electrocatalysis. Nat. mater., 11 (2012) 963-969.

[107]. N.-R. Chiou, C. Lu, J. Guan, et al., Growth and alignment of polyaniline nanofibres with superhydrophobic, superhydrophilic and other properties. Nature nanotechnol., 2 (2007) 354-357.

[108]. H. Kim, H. S. Ahn,M. H. Kim, On the mechanism of pool boiling critical heat flux enhancement in nanofluids. J. Heat Transfer, 132 (2010) 061501.

[109]. Z.-H. Liu, L. Liao, Sorption and agglutination phenomenon of nanofluids on a plain heating surface during pool boiling. Int. J. Heat Mass Transfer, 51 (2008) 2593-2602.

[110]. B. Q. Xiao, Y. Yang,X. F. Xu, Subcooled pool boiling heat transfer in fractal nanofluids: A novel analytical model. Chin. Phys. B, 23 (2013) 026601.

[111]. D. W. Zhou, Heat transfer enhancement of copper nanofluid with acoustic cavitation. Int. J. Heat Mass Transfer, 47 (2004) 3109-3117.

[112]. P. Wagener, S. Ibrahimkutty, A. Menzel, et al., Dynamics of silver nanoparticle formation and agglomeration inside the cavitation bubble after pulsed laser ablation in liquid. Phys. Chem. Chem. Phys., 15 (2013) 3068-3074.

[113]. A. R. M. N. Afrooz, S. M. Hussain,N. B. Saleh, Aggregate size and structure determination of nanomaterials in physiological media: Importance of dynamic evolution. J. Nanopart. Res., 16 (2014) 1-7.

[114]. R. Mangal, S. Srivastava, S. Narayanan, et al., Size-dependent particle dynamics in entangled polymer nanocomposites. Langmuir, 32 (2016) 596-603.

[115]. R. Prasher, P. E. Phelan,P. Bhattacharya, Effect of aggregation kinetics on the thermal conductivity of nanoscale colloidal solutions (nanofluid). Nano Lett., 6 (2006) 1529-1534.

[116]. P. Meakin, Formation of fractal clusters and networks by irreversible diffusion-limited aggregation. Phys. Rev. Lett., 51 (1983) 1119-1122.

[117]. D. A. Weitz, M. Oliveria, Fractal structures formed by kinetic aggregation of aqueous gold colloids. Phys. Rev. Lett., 52 (1984) 1433-1436.

[118]. R. De Rooij, A. Potanin, D. Van den Ende, et al., Steady shear viscosity of weakly aggregating polystyrene latex dispersions. J. Chem. Phys., 99 (1993) 9213-9223.

[119]. M. Y. Lin, H. M. Lindsay, D. A. Weitz, et al., Universality in colloid aggregation. Nature 339 (1989) 360-362.

[120]. P. Meakin, Fractal aggregates. Adv. Colloid Interface Sci. , 28 (1988) 249-331.

[121]. C. Kranenburg, The fractal structure of cohesive sediment aggregates. Estuarine Coastal Shelf Sci., 39 (1994) 451-460.

[122]. P. E. Gharagozloo, K. E. Goodson, Aggregate fractal dimensions and thermal conduction in nanofluids. J. Appl. Phys., 108 (2010) 074309.

[123]. L. H. Hanus, R. U. Hartzler,N. J. Wagner, Electrolyte-induced aggregation of acrylic latex. 1. Dilute particle concentrations. Langmuir, 17 (2001) 3136-3147.

[124]. T. Waite, J. Cleaver,J. Beattie, Aggregation kinetics and fractal structure of γ-alumina assemblages. J. Colloid Interface Sci., 241 (2001) 333-339.

[125]. R. Prasher, W. Evans, P. Meakin, et al., Effect of aggregation on thermal conduction in colloidal nanofluids. Appl. Phys. Lett., 89 (2006) 143119.

[126]. A. A. Potanin, R. De Rooij, D. Van den Ende, et al., Microrheological modeling of weakly aggregated dispersions. J. Chem. Phys., 102 (1995) 5845-5853.

[127]. C.-W. Nan, R. Birringer, D. R. Clarke, et al., Effective thermal conductivity of particulate composites with interfacial thermal resistance. J. Appl. Phys., 81 (1997) 6692-6699.

[128]. Gaganpreet, S. Srivastava, Viscosity of nanofluids: Particle shape and fractal aggregates. Phys. Chem. Liq., 53 (2014) 174-186.

[129]. L. de Martín, W. G. Bouwman, J. R. van Ommen, Multidimensional nature of fluidized nanoparticle agglomerates. Langmuir, 30 (2014) 12696-12702.

[130]. M. Bigerelle, H. Haidara, A. Van Gorp, Monte carlo simulation of gold nano-colloids aggregation morphologies on a heterogeneous surface. Mater. Sci. Eng.: C, 26 (2006) 1111-1116.

[131]. M. R. Schroeder, Fractals, chaos, power laws: Minutes from an infinite paradise. 2009, New York: Dover Inc.

[132]. M. Wozniak, F. R. A. Onofri, S. Barbosa, et al., Comparison of methods to derive morphological parameters of multi-fractal samples of particle aggregates from tem images. J. Aerosol. Sci., 47 (2012) 12-26.

[133]. Y. Xi, J. Chen, Y. Xu, Yield stress of fractal aggregates. Fractals, 23 (2015) 1550028.

[134]. Y. F. Xu, H. Jiang, F. F. Chu, et al., Fractal model for surface erosion of cohesive sediments. Fractals, 22 (2014) 1440006.

[135]. M. Son, T. J. Hsu, The effect of variable yield strength and variable fractal dimension on flocculation of cohesive sediment. Water Res., 43 (2009) 3582-3592.

[136]. G. V. Franks, Y. Zhou, G. J. Jameson, et al., Effect of aggregate size on sediment bed rheological properties. Phys. Chem. Chem. Phys., 6 (2004) 4490-4498.

[137]. T. Woignier, J. Reynes, A. H. Alaoui, et al., Different kinds of structure in aerogels: Relationships with the mechanical properties. J. Non-Cryst. Solids, 241 (1998) 45-52.

[138]. D. W. Schaefer, J. E. Martin, P. Wiltzius, et al., Fractal geometry of colloidal aggregates. Phys. Rev. Lett., 52 (1984) 2371.

[139]. A. Roy, E. Perfect, Lacunarity analyses of multifractal and natural grayscale patterns. Fractals, 22 (2014) 1440003.

[140]. X. Ke, S. Xie, Y. Zheng, et al., Multifractal analysis of geochemical stream sediment data in bange region, northern tibet. J. Earth Sci., 26 (2015) 317-327.

[141]. F. Jing, W. Liqiu, Effective thermal conductivity of nanofluids: The effects of microstructure. J. Phys. D: Appl. Phys., 43 (2010) 165501.

[142]. J. C. Cai, B. M. Yu, M. Q. Zou, et al., Fractal analysis of surface roughness of particles in porous media. Chin. Phys. Lett., 27 (2010) 024705.

[143]. R. Liu, Y. Jiang, B. Li, et al., A fractal model for characterizing fluid flow in fractured rock masses based on randomly distributed rock fracture networks. Comput. Geotech., 65 (2015) 45-55.

[144]. E. Perrier, N. Bird, M. Rieu, Generalizing the fractal model of soil structure: The pore–solid fractal approach. Geoderma, 88 (1999) 137-164.

[145]. E. Perfect, R. L. Blevins, Fractal characterization of soil aggregation and fragmentation as influenced by tillage treatment. Soil. Sci. Soc. Am. J., 61 (1997) 896-900.

[146]. P. Xu, A discussion on fractal models for transport physics of porous media. Fractals, 23 (2015) 1530001.

[147]. B. Ghanbarian, A. G. Hunt, T. E. Skinner, et al., Saturation dependence of

transport in porous media predicted by percolation and effective medium theories. Fractals, 23 (2015) 1540004.

[148]. R. Liu, B. Li,Y. Jiang, A fractal model based on a new governing equation of fluid flow in fractures for characterizing hydraulic properties of rock fracture networks. Comput. Geotech., 75 (2016) 57-68.

[149]. S. Krishnamurthy, P. Bhattacharya, P. Phelan, et al., Enhanced mass transport in nanofluids. Nano lett., 6 (2006) 419-423.

[150]. B. B. Mikic, W. M. Rohsenow, A new correlation of pool-boiling data including the effect of heating surface characteristics. J. Heat Transfer 91 (1969) 245-250.

[151]. Y. Hsu, On the size range of active nucleation cavities on a heating surface. J. Heat Transfer, 84 (1962) 207-213.

Table 1. The summaries on the effective thermal conductivity property of nanofluids

Year	Ref.	Nanoparticle			Host media	η (%)	Note
		Type	λ_{av} (nm)	ϕ_p (vol. %)			
1993	[24]	Al$_2$O$_3$	13	4.3	water	30	the thermal conductivity of water-SiO$_2$ system almost never increased
1999	[25]	Al$_2$O$_3$	33	4.3	water	15	transient hot-wire method
	[25]	CuO	35	4	EG	20	transient hot-wire method
2001	[13]	Cu	10	0.3	EG	40	transient hot-wire method
2002	[26]	Al$_2$O$_3$		5	water	20	transient hot-wire method
2002	[27]	SiC	26	4.2	water	15.8	transient hot-wire method, the effect of particle size and shape is considered
			600	4	water	22.9	
2003	[28]	CuO	50	0.4	water	17	Effective medium theory and fractal theory
2003	[20]	Au	3-4	0.00026	water	21	compared to the conductivity of the basic solution at 30 °C
		Ag	10-20	0.001	toluene	16.5	with respect to the conductivity of the basic toluene at 30 °C
2005	[29]	TiO$_2$	-	5	water	33	TiO2 nanoparticles is rod-shapes of 10×40 nm (diameter by length)
		TiO$_2$	15	5	water	30	TiO2 nanoparticles is in spherical shapes of 15 nm
2010	[30]	Al$_2$O$_3$	43	3	water	9.7	at room temperature
2011	[31]	Al$_2$O$_3$	43	0.086	EG	19	Find the Maxwell method over predicts their experimental values
2012	[32]	Al$_2$O$_3$	40-50	0.5	methanol	10.74	transient hot-wire method
		SiO$_2$	10-20	0.5	methanol	14.29	
2013	[33]	Fe$_3$O$_4$	25	0.1	paraffin	20	transient hot-wire method
2014	[34]	Al$_2$O$_3$	36	1.5	EG/water	32.26	base fluids is 20:80% by weight of EG and water mixtures at 60 °C
2016	[35]	TiO$_2$	5	1	water	6.55	heat transfer in microchannel heat sinks
2016	[36]	Cu	50-100	0.2	EG	25	transient hot wire method
		Cu	50-100	0.2	water	35	

1   EG: ethylene glycol; λ_{av} : average diameter of nanoparticles; ϕ_p : Volume fraction;

2   η : Increase ratio for thermal conductivity of nanofluids compared to base fluid.
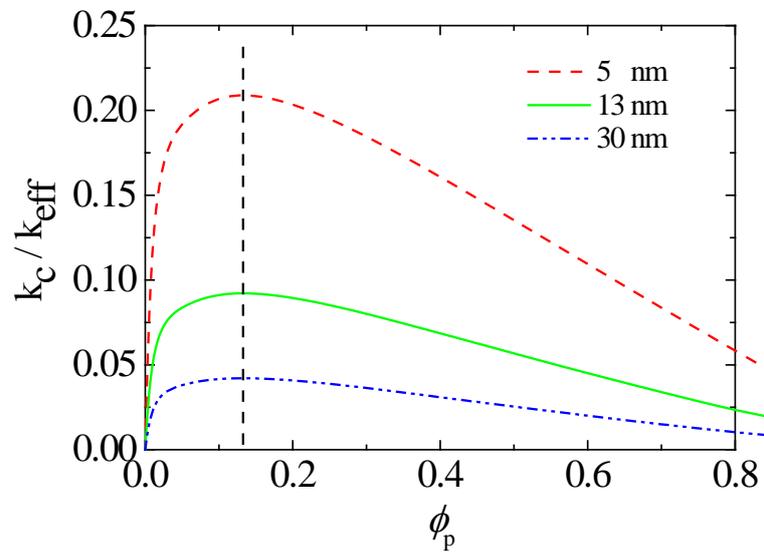
3
4
5
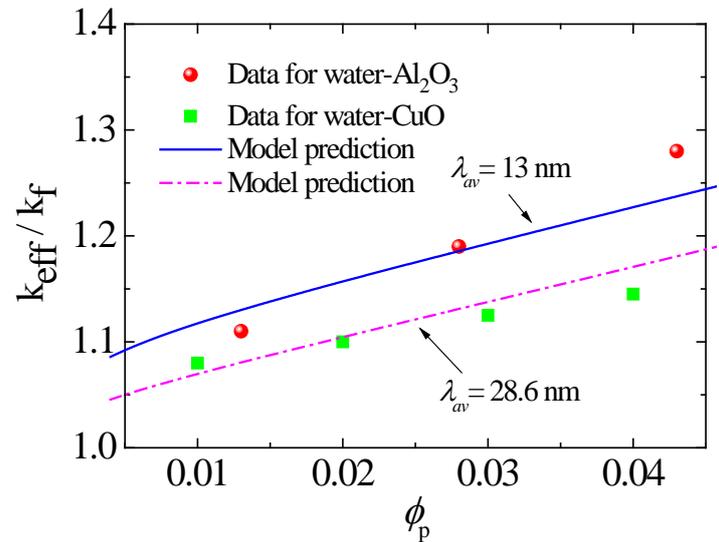
6
7 Figure 1   Test of fractal model (Eq. (20)) for effective thermal conductivity of
8 nanofluids by experiment data (water-Al$_2$O$_3$ [24] and water-CuO [84]). The used
9 parameters: Pr = 6.0, k_f = 0.610 W mK^{-1}, d_f = 4.5×10^{-10} m, c=85, k_p = 46.0 W mK^{-1}
10 and 69.0 W mK^{-1} respectively for Al$_2$ O$_3$ and CuO nanoparticles [57].

11
12
13
14

1
2
3
4
5

6
7 Figure 2   The effects of particle volume fraction and particle size on effective thermal
8 conductivity of nanofluids [57].
9

1
2
3
4
5
6
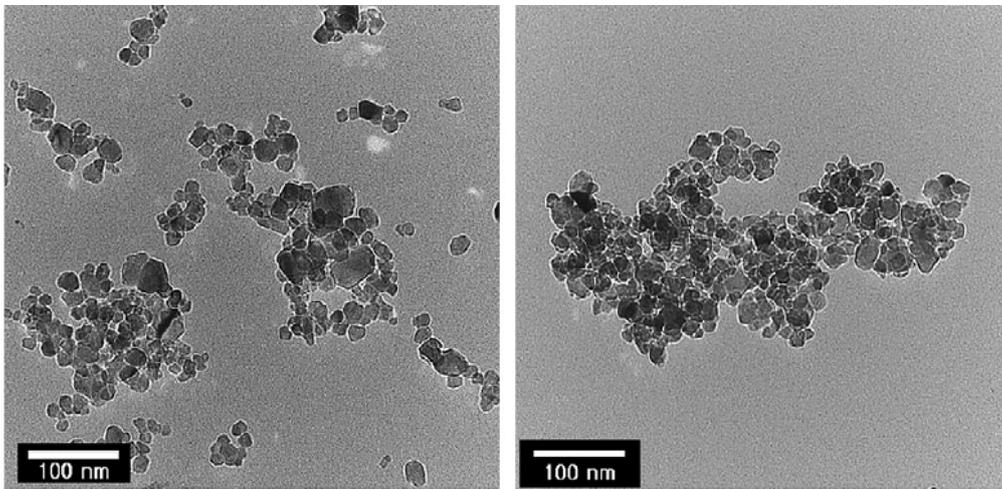
7
8 Figure 3   TEM images of dispersed (Al_2O_3) in distilled water [88]. Copyright
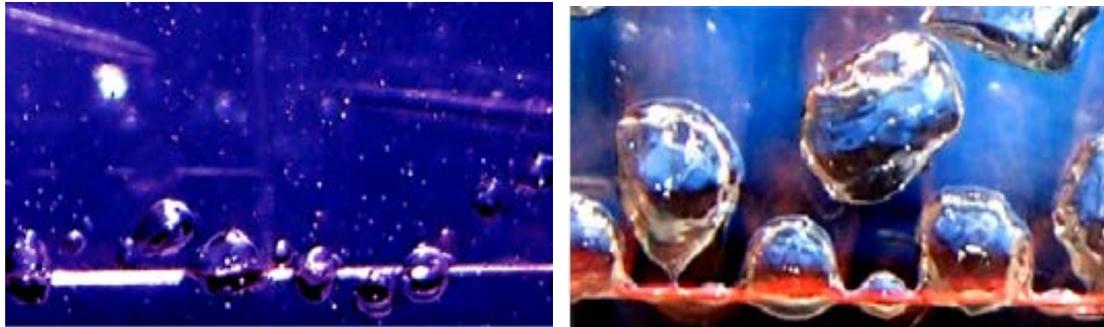9 2007, Elsevier.
10
11

1
2
3
4
5
6

7
8 Figure 4   Comparisons between the FMCHT model predictions and the experimental
9 data for Al_2O_3 nanofluids [95, 96]
10

1
2
3
4
5
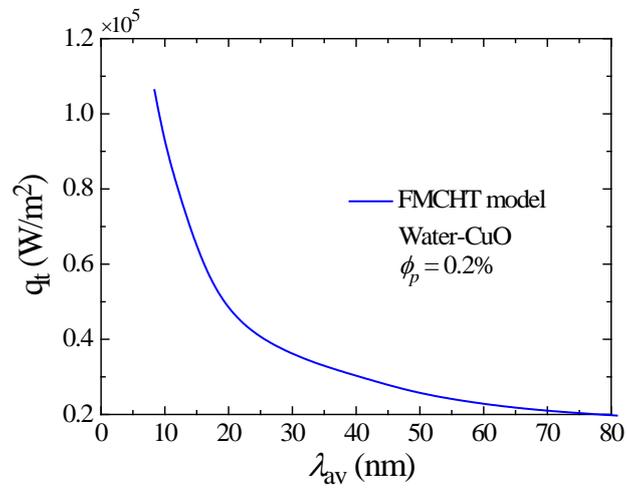
6
7 Figure 5   The heat flux from convective heat transfer of CuO nanofluid versus the
8 average diameter of nanoparticles.
9

1
2
3
4
5
6

(a)

(b)

Figure 6　　SEM micrographs [98] of CHF region in Al$_2$O$_3$ nanofluids (a) $CHF = 0.5 \times 10^6 W / m^2$; (b) $CHF = 1.0 \times 10^6 W/m^2$. Copyright 2007, Elsevier.

$$\times 10^6$$

Water-Al$_2$O$_3$ (λ_{av}= 47nm, ϕ_p= 0.1%)
● Eeperimental data
Water-TiO$_2$ (λ_{av}= 45nm, ϕ_p= 0.1%)
▲ Eeperimental data
Water-SiO$_2$ (λ_{av}= 35nm, ϕ_p= 0.5%)
■ Eeperimental data

q$_t$ (W/m^2)

ΔT (K)
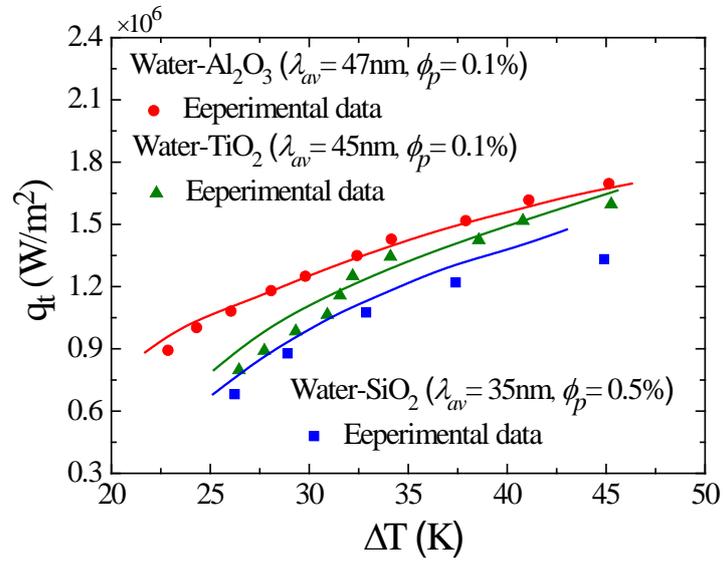
Figure 7   Comparisons of the present FACHF model predictions and the experimental data[108, 109].

1
2
3
4
5
6
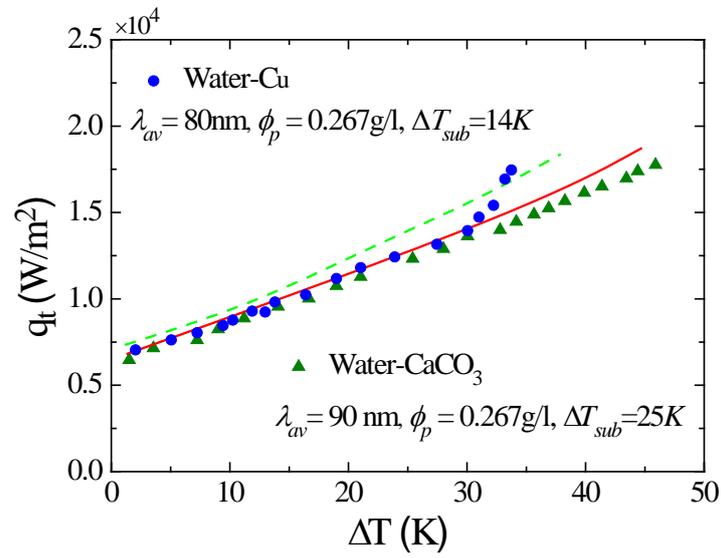
7
8   Figure 8   A comparison between the present model predictions and the experimental
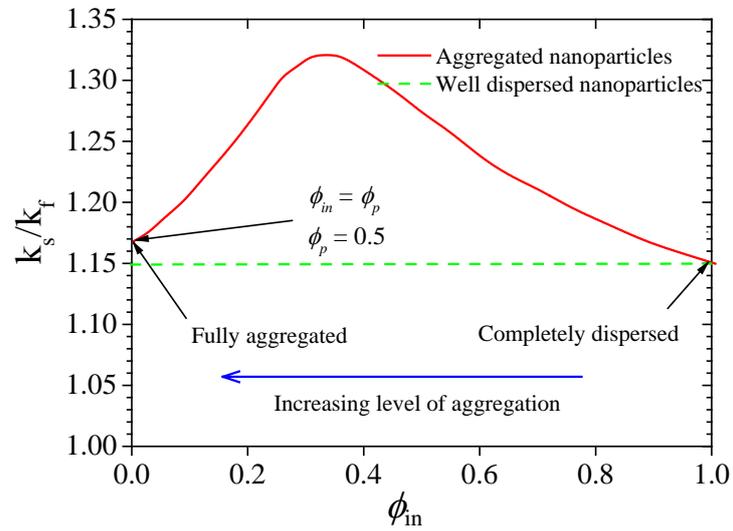9   data for Cu and CaCO$_3$ nanofluids[111].
10

1
2
3
4
5
6
7
8
9
10

0.5 μm
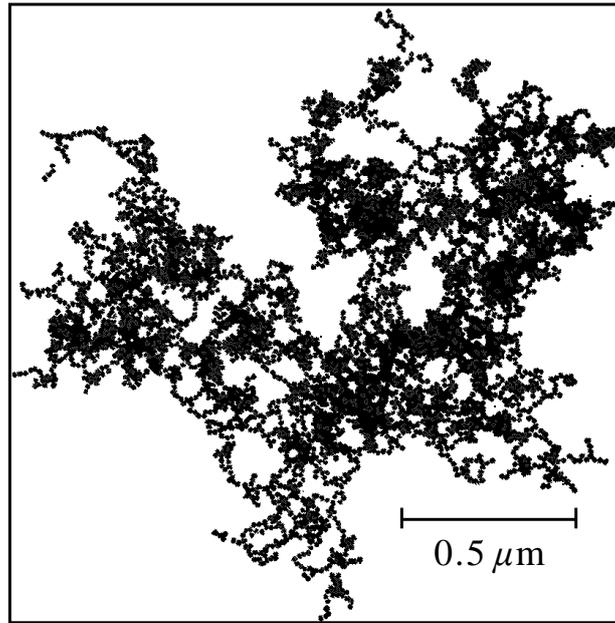
11
12
13 Figure 9   The fractal dimension (1.75) of typical gold colloid aggregate from its TEM
14 image, in which 4739 gold particles are contained[117]. Copyright 1984, American
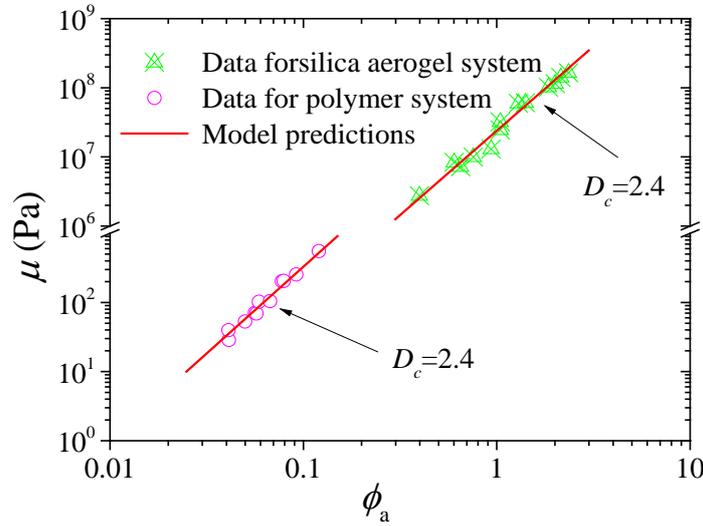15 Physical Society.
16

1
2
3
4
5
6
7

8
9 Figure 10   Effect of aggregation on the conductive contribution to thermal
10 conductivity of nanofluids, compared to that for a well-dispersed system by MG
11 model[115].
12

1
2
3
4
5
6

7
8 Figure 11　　Experimental test on the fractal yield stress model of nanoparticle
9 aggregation versus solid volume fraction[133].
10
11
12